

FliMax, a novel stimulus device for panoramic and highspeed presentation of behaviourally generated optic flow

J.P. Lindemann ^{a,1}, R. Kern ^{a,*,1}, C. Michaelis ^{a,2}, P. Meyer ^a, J.H. van Hateren ^b,
M. Egelhaaf ^a

^a *Lehrstuhl für Neurobiologie, Fakultät für Biologie, Universität Bielefeld, Postfach 100131, D-33501 Bielefeld, Germany*

^b *Department of Neurobiophysics, University of Groningen, Nijenborgh 4, NL-9747 AG Groningen, The Netherlands*

Received 11 September 2002; received in revised form 22 January 2003

Abstract

A high-speed panoramic visual stimulation device is introduced which is suitable to analyse visual interneurons during stimulation with rapid image displacements as experienced by fast moving animals. The responses of an identified motion sensitive neuron in the visual system of the blowfly to behaviourally generated image sequences are very complex and hard to predict from the established input circuitry of the neuron. This finding suggests that the computational significance of visual interneurons can only be assessed if they are characterised not only by conventional stimuli as are often used for systems analysis, but also by behaviourally relevant input.

Keywords: Motion vision; Natural images; Natural stimuli; Optic flow; Self-motion

1. Introduction

The representation of visual information in nervous systems is usually analysed with stimuli that are much simpler than the stimuli experienced by an animal under natural conditions. The differences in the stimuli pertain to both their structural properties which are mainly set by the properties of the outside world as well as to their dynamics which are, at least in actively moving animals, determined to a large extent by the animal's own actions and reactions. In most cases, it is hardly possible to record from visual interneurons in the behaving animal. Exceptions are studies on *Limulus*, where nerve cell recordings were made in almost freely moving animals (Passaglia, Dodge, Herzog, Jackson, & Barlow, 1997), and on monkeys, where the responses of cortical neurons were monitored while the animal looked around in its environment (Vinje & Gallant, 2000, 2002). The

problems with electrophysiological recordings in freely moving animals increase in fast moving, and in particular, in flying ones. A free-flight situation was mimicked by oscillating a fly with an electrode inserted into its brain with dynamics that approximated the rotational self-motion component experienced in free flight (Lewen, Bialek, & de Ruyter van Steveninck, 2001). The latter approach, though technically very demanding, does not take into account the translational component of optic flow generated by self-motion. This limitation does not exist for another recent approach to simulate free-flight situations (Gray, Pawlowski, & Willis, 2002). Behavioural activity was monitored together with multi-neuronal CNS activity in flying moths tethered in a novel flight simulator that combines realistic, interactive visual environments with mechanosensory and olfactory stimuli. Initial experiments reveal that this system is potentially very useful to examine activity from groups of neurons during realistic closed-loop behaviour. Although, with a frame rate of only 60 frames/s, the flight simulator is likely to be too slow for fast flying insects, it appears to be fully appropriate for experiments on moths for which it was developed. To circumvent most of the limitations of previous studies more indirect approaches have recently been employed

* Corresponding author.

E-mail address: roland.kern@uni-bielefeld.de (R. Kern).

¹ The first two authors contributed equally to the project.

² Present address: Innovationskolleg Theoretische Biologie, Humboldt-Universität zu Berlin, Invalidenstraße 43, D-10115 Berlin, Germany.

to stimulate animals with naturalistic image sequences in electrophysiological experiments. In contrast to auditory research where it is comparatively straightforward to use complex natural stimuli for experimental analysis, using naturalistic stimuli in vision research was mainly hampered by technical difficulties to generate and present spatio-temporally complex stimuli. Only recently, some of these obstacles could be surmounted and it has been possible to analyse visual information processing with visual stimuli that approximate to some extent the natural input an animal receives during active locomotion. In several studies image sequences have been presented to the animal in electrophysiological experiments that *might* have been seen by a behaving animal while moving on artificial tracks of locomotion that were designed by the experimenter (Kern, Lutterklas, & Egelhaaf, 2000; Pikel, Lappe, Bremmer, Thiele, & Hoffmann, 1996; Sherk & Fowler, 2001).

This 'replay approach' has recently been extended and the retinal image displacements as experienced by moving flies were replayed to fixed animals during nerve cell recordings (Kern, Lutterklas, Peterleit, Lindemann, & Egelhaaf, 2001a, 2001b). This approach suffered so far from the limitation that the behaviourally generated image sequences were replayed with a specially designed video player at a frame rate of 100 Hz on conventional monitor screens. Although this frame rate is much higher than that of conventional video players, it is too slow if rapid image displacements are to be replayed. Such rapid image displacements are elicited, for instance, during rapid flight manoeuvres or during eye, head or body saccades. Therefore, this technique has been applied so far only to walking animals.

Fast moving animals and, in particular, rapidly flying insects or birds pose several challenges to the generation of behaviourally generated visual stimuli. (i) The retinal images may be displaced so rapidly that temporal aliasing may emerge, if the stimuli are presented on a monitor screen and if the frame rate is not sufficiently high. (ii) The temporal resolution, in particular, of insect eyes is frequently much higher than the temporal resolution of, for instance, human eyes. As a consequence, the stimulus device is required to present image sequences at a very high frame rate to prevent the neuronal responses from time-locking to the individual frames. (iii) Insects and most birds, but also many mammals have almost panoramic visual fields. Moreover, visual interneurons have been found in a variety of animal groups that integrate global information from large parts of the visual field, for instance, in the context of optic flow processing. In addition, synaptic interactions between cells enlarge the classical receptive field of cells even to the contralateral side of the visual field. Conventional stimulus monitors, thus, cover at best a small part of a cell's receptive field (reviews: insects: Egelhaaf, Kern, Krapp, Kretzberg, & Warzecha, 2002;

Hausen & Egelhaaf, 1989; birds: Frost & Wylie, 2000; rabbits: Simpson, 1984).

To meet these challenges and to analyse the neuronal processing of natural stimuli generated by rapidly moving animals we developed a panoramic visual stimulator, called *FliMax*. *FliMax* solves a principal problem of visual stimulation with cathode ray tube (CRT) displays. These displays generate an image on a surface of fluorescent pigments by repeatedly activating the fluorescence with an electron beam. To allow for fast image changes, the fluorescence must dim out within the interframe interval. As a consequence, the image on a CRT is flashing at the frame rate even if a constant image is shown. In contrast, a constant image on *FliMax* does not show any measurable changes in brightness over time.

With an update rate of image frames of 370 Hz *FliMax* is sufficiently fast even for adequately stimulating the eyes of fast flying insects. The present account introduces this novel stimulus device and provides first electrophysiological results on motion-sensitive neurons stimulated with optic flow generated during rapid flight. The experiments were done on the blowfly, because it served during the last decades as a prominent model system for analysing the neuronal mechanisms underlying visual motion processing (Borst & Haag, 2002; Egelhaaf et al., 2002; Egelhaaf & Warzecha, 1999; Hausen & Egelhaaf, 1989). Hence, the fly represents a model animal, where there is sufficient knowledge available on the performance of its visual system which, thus, may serve as reference for an understanding of the processing of complex natural optic flow.

2. Methods

2.1. Design principles of *FliMax*

A VGA card outputs the image information repeatedly at a fixed *frame rate*. In CRT displays this information is used to visibly *refresh* the fluorescent image on the screen. In *FliMax* the refresh of information is invisibly done in the electronics (see below) and we refer to this as *update* of the image. If the image information changes between adjacent frames, we call this *exchange*.

FliMax is designed as a special purpose VGA output device. A standard VGA graphics card is programmed by specific driver code to generate frames at the high temporal resolution of 370 Hz. The VGA signal is interpreted by *FliMax* as an update of the luminance of individual light emitting diodes (LEDs). The luminance of each LED is kept constant between updates by sample-and-hold circuits. These circuits eliminate the flashing characteristic of standard CRT displays.

2.1.1. Geometric design

An ideal stimulator should present the images on a spherical surface with image elements located at equidistant positions to the animal situated in the centre of the sphere. However, the most convenient layout for electronic circuits are flat printed circuit boards (PCBs). *FliMax* approximates a sphere by its icosahedric design (radius of inscribed sphere 0.224 m) (Fig. 1). It consists of 14 of the 20 triangles of an icosahedron each of which forms a PCB. *FliMax* is open at its rear to mount an animal in the centre of the icosahedron and to make recordings from its brain. For electronics purposes the 14 triangular PCBs are combined to seven rhomboids. Each rhomboid holds 1024 equidistantly mounted LEDs (WU-2-53GD, Vossloh Wustlich Opto, Germany) arranged in 32 rows by 32 columns, facing the inner side of *FliMax*. The diameter of the round LEDs is 5 mm, the emitting wavelength is 567 nm, the angle of emittance as specified by the vendor is 60°. However, measurements on individual LEDs indicate only 25° (full width at half maximum) emittance angle. The spatial angular separation of LEDs in the centre of a

triangle as seen from the centre of *FliMax* is about 2.3°. Towards the edges of the board the angular separation between LEDs decreases to minimally 1.5°.

2.1.2. Electronics of *FliMax* timing

The VGA graphics card (Diamond Stealth S540 PCI) generates five signals that are interpreted by the *FliMax* electronics (Fig. 2). The vertical sync pulse marks the beginning of an update cycle, the horizontal sync pulse controls a row switch and the analog “blue” colour signal acts as a pixel clock. The device operates at 370 updates per second. The 14 triangles are updated in a fixed, but pseudo-random order. The update direction of the rows is different for each rhomboid. Therefore, no global apparent movement is generated during an update. The analog “green” and “red” colour signals jointly encode the luminances of a pair of LEDs at each tick of the pixel clock. The maximum luminance averaged over the array of LEDs was 420 cd/m².

Programmable logic circuits (Gate Array Logic, GAL) are employed to generate LED addresses from the sync pulses and the blue colour signal. The GAL chips “enable” the seven rhomboids sequentially (one by one) and generate row (1...32) and column (1...16) addresses used by four subsequent analog demultiplexers. The column demultiplexers assign the “red” and “green” signal to individual neighbouring columns of LEDs. The column demultiplexing is done by CMOS chips (16:1 analog mux/demux CD 4067). The row selection is done by demultiplexers that drive individual CMOS switches (Maxim MAX4501EUK-T) associated to each LED (for details see Fig. 2). To avoid acceptance errors of the red and green analog signals, respectively, the clock signal is transformed into a strobe signal by an appropriate circuit.

Each LED is driven by a small sample-and-hold circuit, that ensures that the voltage at the LED is kept constant between exchanges. During the updates of an LED, the capacitor of the circuit is charged to the voltage of the VGA signal. The capacitor’s voltage acts as the input to a current amplifier (DMOS BS870, General Semiconductor) driving the LED.

2.1.3. Replay-software

Based on standard VGA mode 13h (320 × 200 pixels, 1 Byte = 256 palettised colours) the graphics card is programmed to run at 370 Hz frame rate with the frame size set to 128 × 228 pixels. For each of the 3584 pairs of LEDs updated synchronously we use 8 successive Bytes in video memory rather than 2 Bytes. This measure reduces the effective pixelclock from 14 MHz to 3.5 MHz, extending the time available to charge the sample-and-hold capacitors. In addition, strobing is used to avoid acceptance errors (see above). Each Byte in the video memory is divided by the software into four domains. One bit codes for the “blue” clock signal, three bits

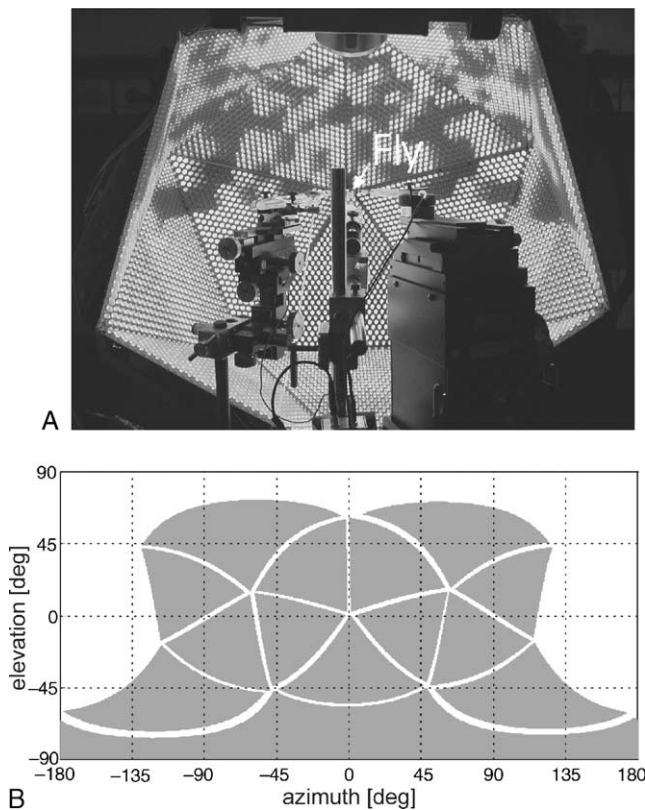


Fig. 1. (A) Photograph of *FliMax* from behind. In the foreground the micromanipulators can be seen by which recording electrodes are inserted into the fly’s brain. (B) Mercator plot of the regions of the visual field that are stimulated (indicated in grey). The white lines between the grey areas indicate the edges of the triangular printed circuit boards. Note that the distortions are a consequence of the Mercator projection.

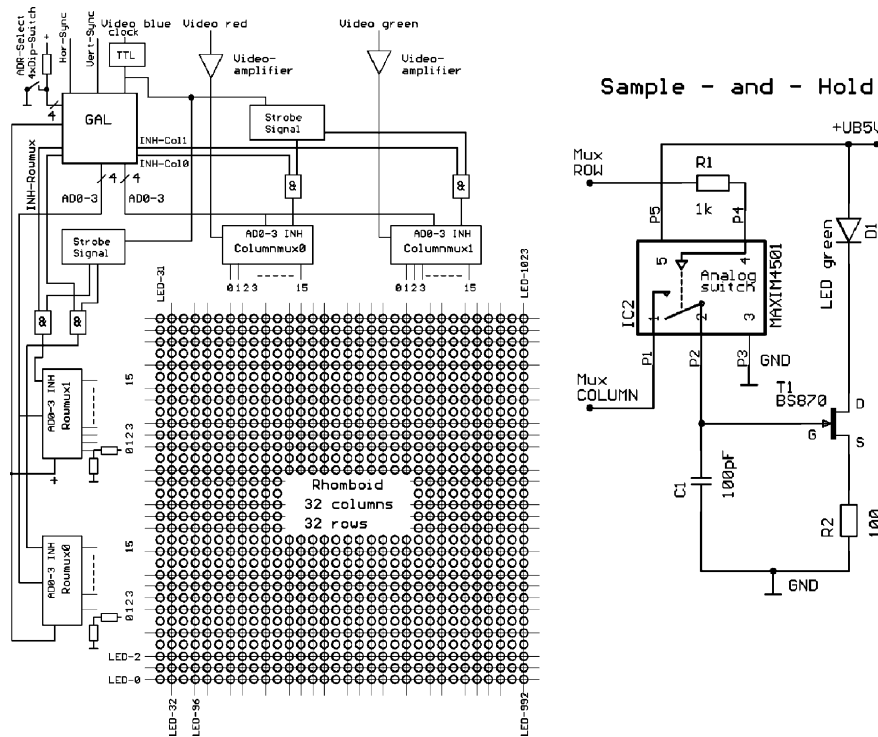


Fig. 2. Logic circuit used to generate LED addresses from the sync pulses and the blue colour signal of a VGA graphics adaptor. The column multiplexers connect the green and red signal to the column wires selected by the column address. The row multiplexers set the row wire selected by the row address to a constant positive voltage every time the strobe signal is active. A CMOS switch and a sample-and-hold circuit (inset) are placed at each crossing of wires in the schematic. The CMOS switches controlled by the active row wire connect the sample-and-hold circuits to the column wires. The sample-and-hold circuits placed at a crossing of active column and row wires sample the signal, all other LEDs are unchanged in brightness, because either the associated CMOS switch or the column multiplexer disconnect the sample-and-hold circuit from the input signals.

encode the luminance of the LED assigned to the green colour signal, another three bits encode the luminance of the LED assigned to the red colour signal. The remaining bit is not used. Eight out of 64 values from the palette are used. They have been chosen to correct for the non-linear voltage vs. brightness characteristics of the LEDs. Hence, about equally sized changes in brightness for each count in the (colour signal) intensity value are obtained.

After the VGA adaptor is initialised to the appropriate resolution and frame rate, the replay can be done by just updating the video memory for each vertical sync period. The video memory is updated incrementally under software control according to frame differences stored in an flic file (animation file format; Kent, 1993). A signal on the printer port is set during video memory updates, sampled at a rate of 4 kHz (I/O-card DT3001, Data Translation) and stored for further reference with respect to timing.

2.1.4. Determination of trajectories

2.1.4.1. Walk trajectories. Flies walking in an arena (diameter: 0.5 m, height: 0.3 m) were video-recorded (50 Hz). The walls of the arena were covered with random textures while the floor was homogeneously white.

Textured objects were introduced into the arena. The video sequences were digitised. The position of the head and the orientation of the flies were automatically determined in each frame by specifically designed software (further details see (Kern et al., 2001b)).

2.1.4.2. Flight trajectories. The position and orientation of the head of flies flying in a textured box (size: 0.4 m \times 0.4 m \times 0.4 m) was measured at 1 kHz using small sensor coils mounted on the head (Fig. 6; for details see (Schilstra & van Hateren, 1998, 1999; van Hateren & Schilstra, 1999)).

2.1.5. Stimulus reconstruction

Both the 3D-trajectory of a behaving fly and the spatial layout of the setup used in the behavioural experiments are known. To reconstruct the visual input of the behaving fly, a 3D-model of the setup is generated (Open Inventor, Silicon Graphics). The trajectory is resampled with a sampling rate of 2220 Hz, i.e. six times the presentation rate of *FliMax*. For each position in the trajectory 14 flat images are rendered by perspective projection to planes parallel to the 14 triangles of *FliMax*. In this way, 14 cameras, each pointing to the centre of one triangle, are simulated. The rendering is

done using Open Inventor and the Mesa (<http://www.mesa3d.org>) OpenGL (SGI) implementation.

In order to reduce spatial aliasing and discretisation artefacts (see below) 2D Gaussian filters are applied to the green colour channel of the resulting RGB images. The red and blue colour channels are not used any further. The centres of the filters correspond to the centres of the LEDs on the triangle. All filters have the same width which approximates the spatial resolution of the blowfly eye (Petrowitz, Dahmen, Egelhaaf, & Krapp, 2000; Smakman, van Hateren, & Stavenga, 1984), i.e. their width at half-maximal amplitude is 1.75° .

The sixfold oversampling of the trajectory is then removed by averaging the filter output for each LED position over six time-steps. This measure results in the proper motion blur, given the frame rate of the *FliMax*, in those parts of the image that contain high image velocities. It thus prevents temporal aliasing, and only introduces a blur not significantly adding to the subsequent blur due to the temporal integration of fly photoreceptors.

For each reconstructed image the (green) intensity values are converted to the video memory format. This conversion includes the reduction of brightness resolution from 256 to 8 intensity steps (3 bits). Simulations using a model of fly photoreceptors (van Hateren & Snippe, 2001) and a preliminary model of fly LMCs (second order neurons presumably in the motion pathway) indicated that the 3-bit discretisation could cause flickering artifacts at moving edges and textures. These effects are reduced to a negligible level by two measures. First, the image is spatially preblurred (see above). Second, the brightness of an LED is toggled between two neighbouring values in consecutive frames, if the correct brightness value is close to the mean of these values. Subsequent temporal integration of these toggled values by the fly's peripheral visual system increases the number of effectively representable brightness values, i.e. the effective brightness resolution, by one bit. To avoid the introduction of wide-field flicker, neighbouring LEDs in each row are toggled out of phase. The toggling halves the temporal resolution of the least significant bit of the device, but the model simulations suggest that this additional flickering is not transferred by the peripheral visual system further down the fly's motion pathway.

2.2. Experimental analysis

2.2.1. Animals and electrophysiological recording

All experiments were done on female blowflies of the genus *Calliphora*. The animals were bred in our laboratory culture. To avoid in-breeding, the culture was refreshed several times a year with animals caught in the wild. The dissection of the 1- to 2-day-old animals for electrophysiological experiments followed the routines conventionally used in our laboratory (see e.g. Warze-

cha, Egelhaaf, & Borst, 1993). Alignment of the flies' eyes with the stimulus device was achieved according to the symmetry of the deep pseudo-pupil (Franceschini, 1975).

Intracellular recordings from the HSE-cell in the right optic lobe were made using electrodes which were pulled from borosilicate glass (GC100TF10, Clark Electro-medical) on a Brown-Flaming Puller (P-97, Sutter Instruments). Filled with 1M KCl they had resistances between 30 and 60 M Ω . Recordings were made with standard electrophysiological equipment. The data were low-pass filtered (corner frequency 2.4 kHz) and sampled at a rate of 4 kHz (I/O-card DT3001, Data Translation) using the VEE Pro 5.0 (Agilent Technologies) in conjunction with DT VPI (Data Translation) software. The HSE-cell was identified by its response mode, its preferred direction of motion and the location of its receptive field (Hausen, 1982a, 1982b). *FliMax* allows us to use standardised stimuli for cell identification and therefore may eliminate the need for hand held probes for this procedure. Experiments were done at temperatures between 28 and 32 °C measured close to the position of the fly in the centre of *FliMax*. Data analysis was done with MatLab 6.0.

2.2.2. Stimulation program

Three different types of visual stimuli were presented sequentially during an experiment: (i) horizontal clockwise and counter-clockwise motion of a vertical sinusoidally modulated grating pattern (wavelength 20° , temporal frequency 2 Hz, contrast 0.98; azimuth: $\pm 120^\circ$ at the eye equator, elevation approximately $\pm 50^\circ$), (ii) optic flow induced on the eyes of a walking fly, (iii) optic flow induced on the eyes of a flying fly. The stimulation protocol, repeated as often as possible, was as follows: 1 s with all LEDs lit at half the maximum brightness, 0.5 s fading of LEDs brightness to the values corresponding to the first frame of the subsequently replayed reconstructed image sequence, 3.4 s replay of one of the three types of image sequences, 7 s interstimulus interval with all LEDs lit at the mean brightness calculated from the flight stimulus. The interstimulus interval ensured that subsequent motion stimulations did not influence each other.

FliMax covers large parts of the fly's visual field. As can be seen in the Mercator plot shown in Fig. 1B, mainly the rear of the animal is not covered by the stimulus. However, virtually the entire ipsi and contralateral receptive field of the HSE-cell that is analysed here is covered (Hausen, 1982b; Krapp, Hengstenberg, & Egelhaaf, 2001).

3. Results

The HSE-cell is an output neuron of the visual system and believed to be involved in providing relevant visual

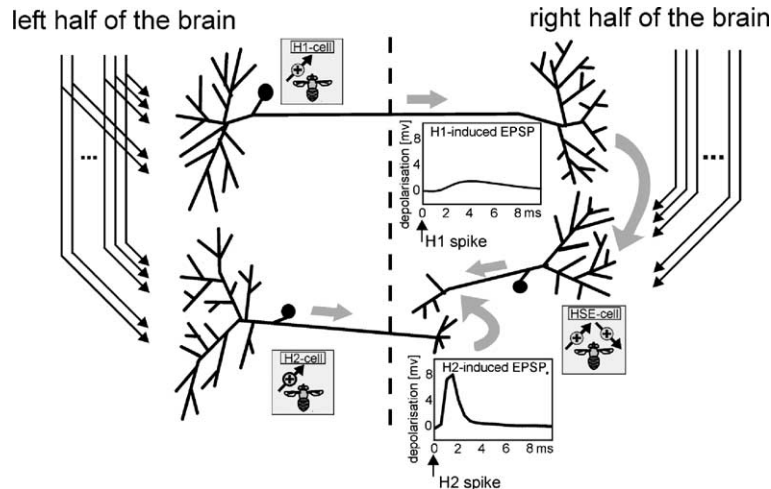


Fig. 3. Input organisation of the HSE-cell of the blowfly. The HSE-cell receives input from the eye ipsilateral to its main dendrite from many retinotopic motion-sensitive elements. As a consequence of this input, the HSE-cell is depolarised by front-to-back motion and hyperpolarised by back-to-front motion. The HSE-cell receives additional input on its main dendrite from the H1-cell or close to its axon terminal from the H2-cell. The spike activity of H1 and H2 is increased during back-to-front motion in the contralateral visual field and elicits EPSPs in HSE (see insets). As a consequence of its input organisation the right HSE-cell can be expected to be depolarised during counter-clockwise rotations of the fly and hyperpolarised during rotations in the opposite direction.

information that is used in course control. The HSE-cell receives retinotopic input from the eye ipsilateral to its main dendrite (Fig. 3). As a consequence, it is excited by ipsilateral front-to-back motion and inhibited by back-to-front motion. Moreover, it receives excitatory input on its main dendrite from the contralateral H1-neuron as well as close to its output terminal from the contralateral H2-cell (Haag & Borst, 2001; Horstmann, Egelhaaf, & Warzecha, 2000). Since both H1- and H2-neuron are excited during back-to-front motion, the HSE-cell in the right half of the brain can be expected to be excited by optic flow generated during counter-clockwise rotations of the animal about its vertical body axis and to be inhibited during rotations in the opposite direction (Fig. 3).

3.1. Conventional wide-field gratings

Conventional grating stimuli were used for experimentation to test whether the responses obtained with *FliMax* differ in any obvious way from those obtained with stimulus devices used in previous studies, such as mechanically moving drums or monitor screens. Fig. 4 displays a sample record of an HSE-cell response to constant velocity motion in the preferred direction and subsequently in its null direction. The record shows the typical features of HSE-cell responses: They are characterised by graded de- and hyperpolarisations relative to the resting potential. On average, the depolarisation during preferred direction motion is 15.2 mV ($N = 12$) and the hyperpolarisation during null direction motion is -8.4 mV ($N = 12$). These values are in the range of

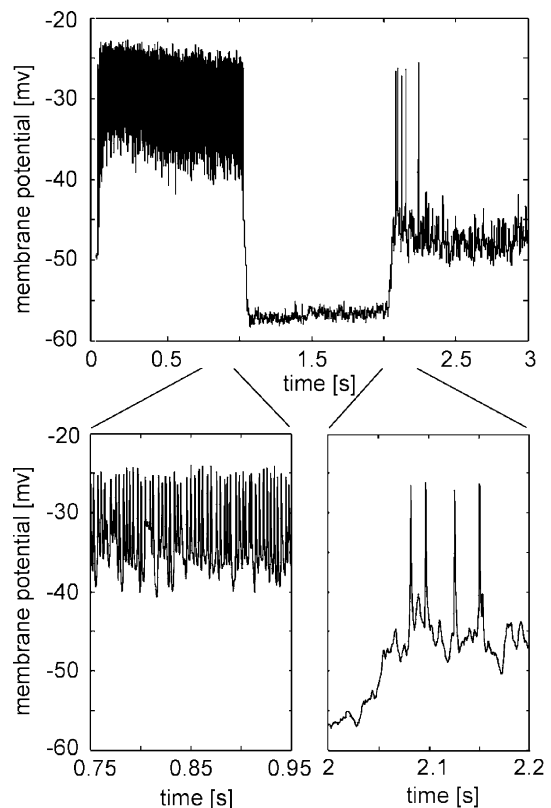


Fig. 4. Responses of the HSE-cell to grating patterns moving initially at a constant velocity for one second in the cell's preferred direction and then for another second in the null direction. During the last second the pattern is stationary. The graded depolarisations during preferred direction motion are superposed by small-amplitude spike-like depolarisations (see also bottom diagrams). The spike-like depolarisations are large when they are generated as rebound spikes after a hyperpolarisation of the cell (bottom right).

responses that were published in earlier accounts (Hausen, 1982b).

Rapid spike-like depolarisations superimpose the graded depolarisations. These spikelets vary in amplitude to a large extent. They may hardly be discerned in some preparations, but they may also reach amplitudes of full-blown spikes in other preparations. Spikelets superimposed on large graded depolarisations tend to be smaller than those generated at the resting level of the cell as, for instance, just after the release from hyperpolarisation elicited by null direction motion (Fig. 4). These features of spikelets are well documented (Haag & Borst, 1998; Hausen, 1982a) and the consequence of the activation and inactivation properties of voltage-dependent sodium channels (Haag, Theunissen, & Borst, 1997; Hengstenberg, 1977).

In conclusion, as judged by the responses to classical grating patterns *FliMax* appears to be fully appropriate as a visual stimulation device.

3.2. Optic flow generated by walking flies

The membrane potential of HSE-cells fluctuates in a complex manner when the cell is stimulated with image sequences as are seen by a fly walking around in its environment. The characteristics of the membrane potential fluctuations elicited by behaviourally generated optic flow and what they may encode about the animal's self-motion and/or the layout of the surroundings have been analysed in previous accounts. It was concluded that the HSE-cell encodes the direction of turns of the walking animal largely independent of the spatial layout and texture of the environment. Only when the animal is very close to an object, the neuronal responses are affected by it (Kern et al., 2001a, 2001b). These previous analyses were limited by the fact that image sequences were presented on a monitor screen that covered only part (though a large one) of the cell's receptive field. All displays with a cathode ray tube (CRT) do not show a still image but iteratively flash each pixel at the frame rate. In contrast, *FliMax* presents a constant image between differing updates as long as the image does not move. Moreover, for technical reasons stimulation was based in our previous studies on a 100 Hz video player (Kern et al., 2001b). Although the frame rate was much higher than that of conventional video players, it led to some time-locking of the neuronal response to the frame rate. With *FliMax* we now test whether the responses of HSE-cells may differ when they are elicited by the same image sequences. The responses will be related, as in our previous studies (Kern et al., 2001a, 2001b), to the rotational velocity component of the optic flow generated by yaw movements of the fly.

Image sequences generated by walking flies were presented to the same set of flies in two alternative ways:

(i) The device was operated at an update rate of 370 per second, but the images were exchanged, as in our earlier experiments with a computer monitor, at 100 exchanges per second; this procedure implies that each frame was presented 3–4 times. (ii) The device was operated at an exchange rate of 370 per second. The image sequences were linearly interpolated so that image exchanges could be done at a rate of 370 frames per second.

As is obvious from the examples shown in Fig. 5C and D the time course of the responses to both types of image sequence are virtually the same. Moreover, these responses do not differ in any pronounced way from the time course of the responses that were obtained in our previous study with a monitor screen as stimulus device (compare traces in Fig. 5B with C and D). Only the overall response amplitudes that were obtained with *FliMax* are somewhat larger than those obtained with a conventional stimulus device. Notwithstanding, this comparison shows that the general results of our previous study are still valid and that the same conclusions as were drawn in the previous study would have been drawn on the basis of the improved visual stimulator.

Despite these similarities on the time scale at which the responses were analysed in our previous study, the temporal structure of the responses on a time scale of milliseconds depends on the way the image sequences were presented. This feature can be seen in the power spectra of the responses (Fig. 5B–D, bottom row). As is characteristic of fly HS neurons (Haag & Borst, 1997; Warzecha, Kretzberg, & Egelhaaf, 1998) the responses contain most of their power at frequencies below 10 Hz. The attenuation of high-frequency components is a consequence of time constants that are an inevitable constituent of movement detectors (Egelhaaf & Borst, 1993). However, the power spectrum of the responses obtained in our previous study with stimuli generated on a monitor screen reveals pronounced peaks in the power spectrum at 100 Hz, i.e. at the refresh rate of the monitor as well as the exchange rate of the image frames, and at higher harmonics of this frequency (Fig. 5B, lower panel). These peaks are much reduced when the same image sequences are shown without CRT flashing, but still at an exchange rate of 100 Hz (Fig. 5C, lower panel). This finding suggests that the time-locking of the neuronal responses has to be attributed mainly to the flashing of conventional monitors and not so much to the rate of the image exchange. When the frame exchange rate is increased to 370 Hz, the maximum that is possible with *FliMax*, no distinct peak is discernible at this frequency in the power spectrum or at half this frequency (Fig. 5D, lower panel), which is the resulting frequency for the least significant bit (see Section 2).

These findings allow us to draw the following conclusions. (i) Even if the responses time-lock to the update and/or frame rate of the motion stimulus on a fine

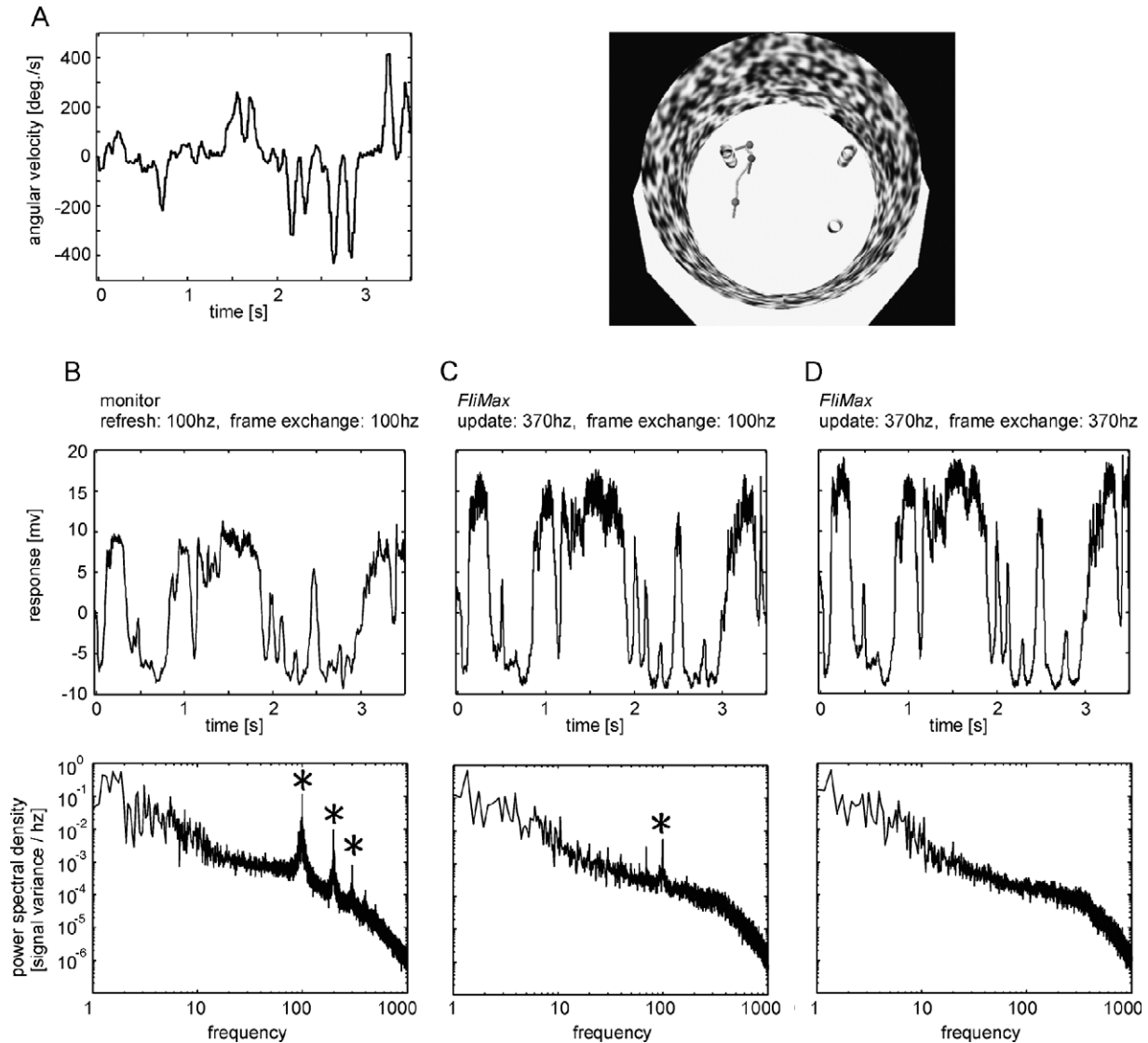


Fig. 5. Responses of the HSE-cell to behaviourally generated optic flow as experienced by a walking fly. (A) Angular velocity of the fly as a function of time (left) and walking track within the arena (right). The orientation of the fly's body axis is shown only at three instants of time; positive (negative) values denote counter-clockwise (clockwise) turns. (B) Section of the average response of 8 HSE-cells stimulated with a computer monitor at a frame rate of 100 Hz (upper diagram) (Data taken from Kern et al. (2001b)). Average power spectrum of individual response traces have a pronounced peak at 100 Hz and at integer multiples of this frequency (see asterisks; bottom diagram). (C) Average response of 15 HSE-cells stimulated by *FliMax* at a rate of 370 Hz; the effective image exchange rate was 100 Hz (upper diagram). The corresponding average power spectrum of the individual response traces has a peak at 100 Hz which is, however, much smaller than the peak shown in B (bottom diagram). (D) Average response of 11 HSE-cells stimulated by *FliMax* at a rate of 370 Hz; the image exchange rate was 370 Hz (upper diagram). The corresponding average power spectrum of the individual responses does not show any obvious peak at 100 Hz or 370 Hz (bottom diagram).

time scale, the responses are virtually indistinguishable on a coarser time scale, (ii) Exchange rates of 185/370 Hz as are possible with *FliMax* are fully appropriate to elicit the illusion of smooth motion in fly motion sensitive neurons.

3.3. Optic flow generated by flying flies

The membrane potential of the HSE-cell fluctuates much in response to image sequences generated during free flight (Fig. 6). The membrane potential fluctuations

appear to be, at least for some sections of the flight, faster than those induced while the animal is walking. This might be the consequence of the angular velocity and frequency of head and body rotations (Schilstra & van Hateren, 1999; van Hateren & Schilstra, 1999) being often considerably higher during flight than when the animal is walking. As the profile of head angular velocity (Fig. 6B) indicates the animal executes a sequence of rapid saccadic turns about its vertical body axis. During saccades the head may reach angular velocities of about 3000°/s. Between saccades the animal flies rel-

actively straight, i.e. angular velocities are relatively small (Schilstra & van Hateren, 1999). The overall optic flow as projected onto the receptive field of the HSE-cell and

weighed according to the local preferred direction and sensitivity of the cell (Krapp et al., 2001) is largely dominated by its angular velocity component. The

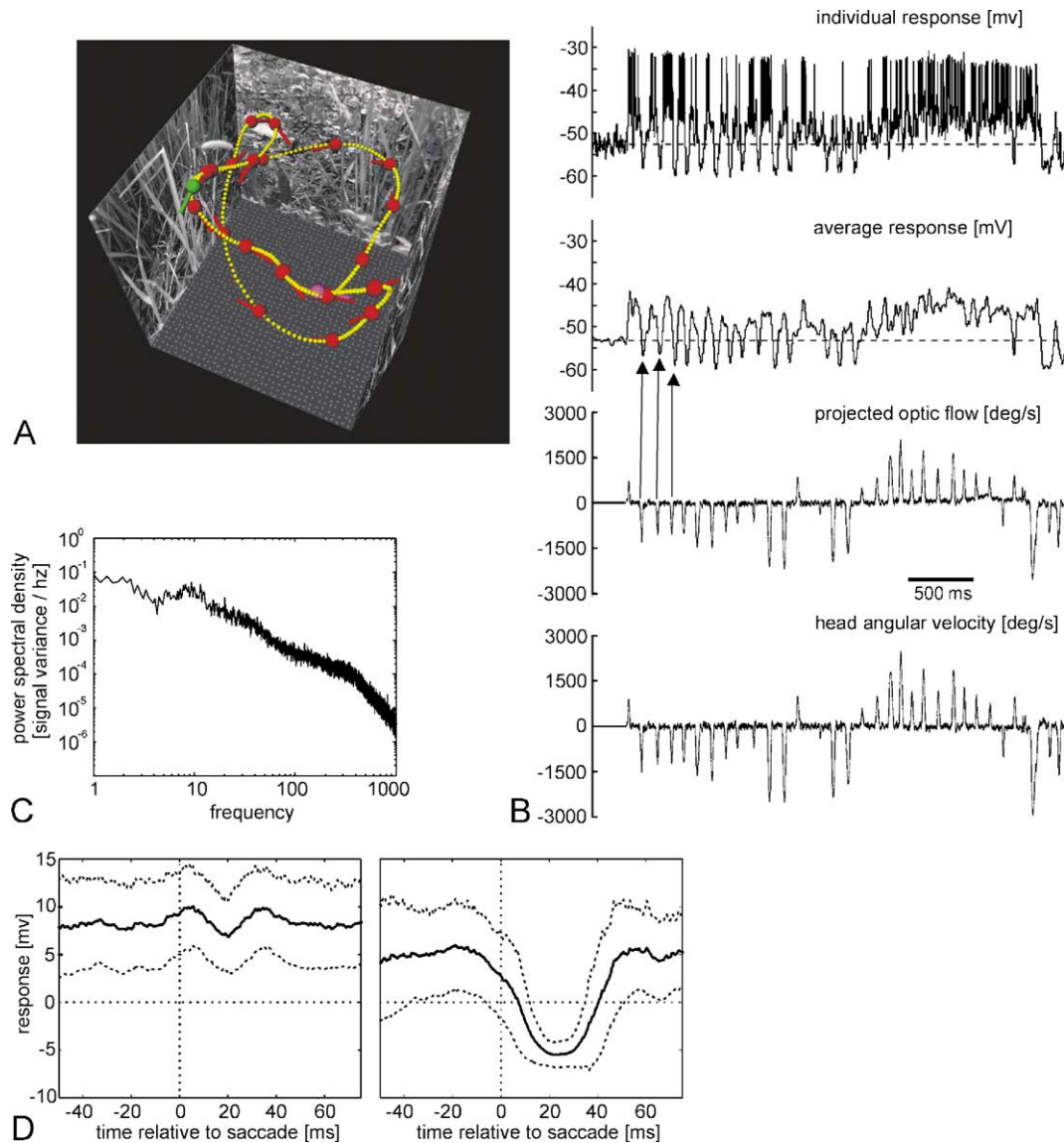


Fig. 6. Responses of the HSE-cell of a blowfly to behaviourally generated optic flow as experienced during a free-flight manoeuvre. (A) Flight trajectory monitored in a cubic cage ($0.4 \times 0.4 \times 0.4 \text{ m}^3$) covered on its side walls with images of herbage. The position of the fly is shown by small spheres every 10 ms. The position and orientation of the head are shown every 130 ms; the starting position is indicated by the green 'fly', the end position by the magenta 'fly'. (B) Responses to behaviourally generated stimuli. Top trace: individual response; HSE responds to motion with graded de- and hyperpolarisations; spike-like depolarisations superpose the graded potential changes. Second trace: average response ($n = 7$), smoothed with a Savitzky–Golay polynomial filter (width 25 ms, polynomial order = 1). Third trace: Optic flow during flight manoeuvre projected on local response field of the right HSE-cell (Krapp et al., 2001). The optic flow is weighed according to the cell's local preferred directions and motion sensitivities. Positive (negative) values denote motion in the cell's preferred (null) direction. In the equatorial part of the eye, the preferred direction of the HSE-cell corresponds to front-to-back motion. Bottom trace: Angular velocity of the fly's head. Sharp angular velocity peaks corresponding to saccade-like turns of the fly dominate the time-dependent angular velocity profile. Positive (negative) values denote counter-clockwise (clockwise) turns of the head in a head-centred coordinate system. In contrast to expectations based on the input organisation of the HSE-cell there are no obvious response peaks during preferred direction motion evoked by counter-clockwise saccades. However, there are pronounced hyperpolarisation going along with clockwise saccades (see arrows). (C) Power spectrum of individual responses of an HSE-cell to image displacements as experienced during free-flight manoeuvres. The power spectrum is mainly flat up to frequencies of about 10 Hz. At higher frequencies the signal power decreases. (D) Saccade-triggered average of the HSE responses ($N = 1$). Counter-clockwise saccades (left) go along with image motion in the HSE-cell's preferred direction, clockwise saccades (right) go along with image motion in the null direction. Zero time corresponds to the maximum angular velocity. The resting potential was subtracted before averaging. 290 saccades from 10 different flight trajectories were evaluated. The optic flow corresponding to each trajectory was replayed between 2 and 7 times.

translational optic flow component is much smaller than the rotational one (compare bottom traces in Fig. 6B).

As judged from its input organisation (Fig. 3), the HSE-cell is expected to respond best to optic flow elicited by rotations of the animal about its vertical body axis. The responses to optic flow experienced by free-flying flies only partly fit this expectation (Fig. 6). The HSE-cell responds with graded depolarisations that are superimposed by spikes almost during the entire flight sequence. Clockwise saccades going along with optic flow in the cell's null direction lead to pronounced hyperpolarisations. The amplitude of the hyperpolarisations does not appear to increase consistently with the saccade amplitude. In contrast to clockwise saccades, counter-clockwise saccades eliciting preferred direction motion do not lead to corresponding depolarisations. This characteristic is not merely due to saturation of the response, because saccades fail to elicit depolarisations even during phases of the flight sequence where the overall depolarisation of the cell is much smaller than the maximal depolarisation level that can be evoked by visual motion (Fig. 6B). As is shown by the saccade-triggered average of the neuronal response, the cell even slightly hyperpolarises as a consequence of counter-clockwise saccades although the optic flow is in the preferred direction of the cell. This hyperpolarisation, however, is much smaller than the one elicited, on average, by saccades leading to image displacements in the null direction (Fig. 6D).

From a technical point of view it is important to note that, in accordance with the results shown in Fig. 5, no distinct peak is discernible in the power spectrum of the neuronal responses at the frame exchange rate of 370 Hz that was used to obtain the responses to optic flow as generated in free flight (Fig. 6C).

In conclusion, the time course of the response of the HSE-cell during complex free-flight manoeuvres is far from being proportional to the time course of the angular velocity or the optic flow as projected onto the receptive field of the cell. Moreover, it is hard to predict the performance of the HSE-cell during complex flight manoeuvres, although its input circuitry and its responses to a wide range of motion stimuli are known in great detail.

4. Discussion

FliMax is a high-speed panoramic visual stimulation device which is suitable to analyse the response properties of visual interneurons even when they have very large binocular visual fields. Rapid image displacements which are characteristic of the natural visual input of fast moving animals can be presented with *FliMax*. It could be shown for an identified motion sensitive neuron in the visual system of the blowfly, the HSE-cell, that its

responses to behaviourally generated image sequences are very complex. These responses cannot easily be predicted from the established input circuitry of the neuron, although its biophysical properties and responses to a wide range of motion stimuli are known in great detail (Borst & Haag, 1996; Haag & Borst, 1996, 1997, 1998, 2000; Haag et al., 1997, 1999; Hausen, 1982a, 1982b; Horstmann et al., 2000; Kern et al., 2000; Warzecha et al., 1998). This finding suggests that the computational significance of visual interneurons can only be assessed if they are characterised not only by conventional stimuli often used for systems analysis, but also by behaviourally relevant input. *FliMax* represents a versatile and useful system which allows us to achieve this goal even in animals with almost panoramic visual fields and fast eyes.

4.1. Methodological considerations

The main difference of *FliMax* to existing LED-based stimulators (Baader, 1991; Strauss, Schuster, & Götz, 1997) is that it directly uses the output of a specially programmed VGA graphics adaptor. This feature is the main trick that enables *FliMax* to reach frame rates of 370 frames per second. This high frame rate is not only necessary because of the high temporal resolutions of insect eyes (reviews: Juusola, French, Uusitalo, & Weckström, 1996; Laughlin, 1994), but also to prevent spatio-temporal aliasing from affecting the neuronal responses to rapid image displacements of relatively fine-grained patterns.

There are several limitations of the special design of *FliMax* that need to be discussed. Although the temporal resolution of *FliMax* is very high, its spatial resolution is relatively poor, because it consists of only 7168 LEDs, corresponding to an angular separation of LEDs judged from the centre of *FliMax* of about 2.3°. This spatial resolution might be adequate for analysing vision of many insects, because the number of LEDs roughly coincides with the number of ommatidia and, thus, retinal sampling points. Although the spatial grid of LEDs that are used for stimulation is much coarser than the spatial resolution of the human eye, a vivid impression of a smoothly moving pattern can be evoked by *FliMax* even in human observers. Hence the electronic principles underlying *FliMax* may well be adapted as a panoramic optic flow stimulator for experiments on a wide range of species including vertebrates.

Another limitation of *FliMax* pertains to the flatness of the printed circuit boards which form the modules of its icosahedral design. Thus, the angle at which the LEDs are seen by the animal in the centre of *FliMax* varies systematically from the centres of the boards towards their edges. As a consequence of the directional emittance characteristics of the LEDs, their apparent brightness decreases concomitantly to about 20% at the

boards' edges relative to the apparent brightness of LEDs in the centre of the board. To check for potential consequences of this feature we covered in control experiments (data not shown) the centre of the LED-triangle with a circular grey filter (radius 5 cm, transmission 20%). This area of the LED-triangle stimulated the most sensitive region of the HSE-cell's receptive field. Although this filter largely affected the brightness distribution within the receptive field of the HSE-cell, the responses to visual motion did not noticeably change. This is consistent with simulations using a model of the fly peripheral visual system (see Section 2), showing that steady spatial gradients are mostly removed by peripheral gain controls. Hence, we conclude that the neuronal responses, at least to optic flow stimuli, are not affected by the brightness gradients that are an inevitable consequence of the flat design of the printed circuit boards in their current form. In future versions of *FliMax* the LEDs might be bent towards the centre of the stimulator.

In contrast to limitations in the spatial details that can be resolved by *FliMax*, there are no functionally relevant limitations with regard to its temporal resolution. Even angular velocities of up to 3000°/s did not lead to aliasing, at least at the relatively coarse spatial resolution at which the environment is seen. Moreover, the neuronal responses of the fly HSE-cell did not time-lock to the image displacements if the frames are displayed at a rate of 370 per second. Since the photoreceptors of flies have a much higher resolution than those of vertebrates it appears to be likely that the temporal resolution of *FliMax* does not represent a limitation for most visual systems.

4.2. Neuronal responses to natural optic flow

We have shown that the responses of the HSE-cell to complex optic flow as may be generated on the eyes in behavioural situations differ from what may be expected on the basis of the wiring diagram of the input circuitry of the analysed neuron. The reason for this finding are most likely non-linearities inherent in optic flow processing.

The mechanisms underlying visual motion detection are inevitably non-linear (Borst & Egelhaaf, 1993; Poggio & Reichardt, 1973). As a consequence of such non-linearities and delay filters the responses of motion sensitive wide-field neurons, such as the HSE-cell, have been shown to depend not only on the angular velocity, but non-linearly also on acceleration and higher-order temporal derivatives of pattern motion (Egelhaaf & Reichardt, 1987). Therefore, the HSE-cell was found to mimic the time course of pattern motion only when it does not change too rapidly (Egelhaaf & Reichardt, 1987; Haag & Borst, 1997). The peculiar features of the neuronal responses of walking and flying flies that were

described here and in previous studies (Kern et al., 2001a, 2001b) may be attributed, at least to a large extent, to the specific dynamical properties of the motion detection system. From a functional point of view it is important to note, although this may be surprising, that both during walking and during flight, the fly's motion vision system apparently does not operate in its linear range, where it faithfully reproduces the time course of pattern velocity. This point needs to be stressed, because it is frequently implicitly assumed that the main task of fly motion sensitive neurons is to reproduce the time course of image motion (Bialek, Rieke, de Ruyter van Steveninck, & Warland, 1991). The present study shows that a priori assumptions of this kind should only be made with some caution and that only on the basis of responses to behaviourally generated stimuli inferences concerning the natural operating range of the system should be made.

The non-linear spatial integration properties of the HSE-cell (Borst, Egelhaaf, & Haag, 1995; Egelhaaf, Haag, & Borst, 1994; Hausen, 1982b; Single, Haag, & Borst, 1997) are likely to be another reason for the deviation of the responses to behaviourally generated optic flow from expectations. Small stimuli already lead to near-maximal responses of the cell. Increasing stimulus size or the number of texture elements does not increase the responses much further. Although this basic feature of fly motion-sensitive neurons is known for long, it has not yet been analysed in which way different objects moving simultaneously at different velocities in different directions in the cell's receptive field may interact to shape the final response of the cell. Hence, it is currently not possible to assess to what extent the complex neural responses to behaviourally generated optic flow depend on the non-linear spatial integration properties of the neuron.

Finally, understanding the responses to natural image flow may be further complicated, because the properties of fly motion-sensitive neurons were shown to change as a result of stimulus history (Borst & Egelhaaf, 1987; de Ruyter van Steveninck, Bialek, Potters, Carlson, & Lewen, 1996; Fairhall, Lewen, Bialek, & de Ruyter van Steveninck, 2001; Harris & O'Carroll, 2002; Harris, O'Carroll, & Laughlin, 1999, 2000; Maddess & Laughlin, 1985). Although the functional significance of these adaptational processes is still debated, they may well play a role in adjusting the operating range of the mechanisms underlying optic flow processing in different behavioural contexts.

In conclusion, as a consequence of non-linearities inherent in visual information processing and the peculiar spatio-temporal properties of natural visual input which may even differ much in different behavioural contexts, it is not possible to make sound predictions on the basis of analyses with conventional stimuli about how a visual system operates under natural conditions.

A versatile and high-speed visual stimulator such as *FliMax* may help to analyse the performance of neuronal circuits under behaviourally relevant stimulus conditions.

Acknowledgements

We would like to thank Udo Witte (computer support), Peter Hunger (electronic workshop) and Ulrich Richhardt (mechanical workshop) for their invaluable help in constructing *FliMax*. Norbert Boeddeker and Rafael Kurtz made valuable suggestions on earlier versions of this manuscript. Supported by the Deutsche Forschungsgemeinschaft (DFG).

References

- Baader, A. (1991). Simulation of self-motion in tethered flying insects: an optical flow field for locusts. *Journal of Neuroscience Methods*, *38*, 193–199.
- Bialek, W., Rieke, F., de Ruyter van Steveninck, R., & Warland, D. (1991). Reading a neural code. *Science*, *252*, 1854–1857.
- Borst, A., & Egelhaaf, M. (1987). Temporal modulation of luminance adapts time constant of fly movement detectors. *Biological Cybernetics*, *56*, 209–215.
- Borst, A., & Egelhaaf, M. (1993). Detecting visual motion: Theory and models. In F. A. Miles, & J. Wallman (Eds.), *Visual motion and its role in the stabilization of gaze*. Amsterdam: Elsevier.
- Borst, A., Egelhaaf, M., & Haag, J. (1995). Mechanisms of dendritic integration underlying gain control in fly motion-sensitive interneurons. *Journal of Computational Neuroscience*, *2*, 5–18.
- Borst, A., & Haag, J. (1996). The intrinsic electrophysiological characteristics of fly lobula plate tangential cells: I. Passive membrane properties. *Journal of Computational Neuroscience*, *3*, 313–336.
- Borst, A., & Haag, J. (2002). Neural networks in the cockpit of the fly. *Journal of Comparative Physiology A*, *188*, 419–437.
- de Ruyter van Steveninck, R., Bialek, W., Potters, M., Carlson, R. H., & Lewen, G. D. (1996). Adaptive movement computation by the blowfly visual system. In: David L. Waltz (Ed.), *Natural and Artificial Parallel Computation: Proceedings of the Fifth NEC Research Symposium*, pp. 1–21.
- Egelhaaf, M., & Borst, A. (1993). Movement detection in arthropods. In J. Wallman, & F. A. Miles (Eds.), *Visual motion and its role in the stabilization of gaze* (pp. 53–77). Amsterdam, London, New York: Elsevier.
- Egelhaaf, M., Haag, J., & Borst, A. (1994). Processing of synaptic information depends on the structure of the dendritic tree. *Neuroreport*, *6*, 205–208.
- Egelhaaf, M., Kern, R., Krapp, H. G., Kretzberg, J., & Warzecha, A.-K. (2002). Neural encoding of behaviourally relevant motion information in the fly. *Trends in Neurosciences*, *25*, 96–102.
- Egelhaaf, M., & Reichardt, W. (1987). Dynamic response properties of movement detectors: Theoretical analysis and electrophysiological investigation in the visual system of the fly. *Biological Cybernetics*, *56*, 69–87.
- Egelhaaf, M., & Warzecha, A.-K. (1999). Encoding of motion in real time by the fly visual system. *Current Opinion in Neurobiology*, *9*, 454–460.
- Fairhall, A. L., Lewen, G. D., Bialek, W., & de Ruyter van Steveninck, R. (2001). Efficiency and ambiguity in an adaptive neural code. *Nature*, *412*, 787–792.
- Franceschini, N. (1975). Sampling of the visual environment by the compound eye of the fly: Fundamentals and applications. In A. W. Snyder, & R. Menzel (Eds.), *Photoreceptor optics* (pp. 98–125). Berlin, Heidelberg, New York: Springer.
- Frost, B. J., & Wylie, D. R. W. (2000). A common frame of reference for the analysis of optic flow and vestibular information. In M. Lappe (Ed.), *Neuronal Processing of Optic Flow* (pp. 121–140). San Diego: Academic Press.
- Gray, J. R., Pawlowski, V., & Willis, M. A. (2002). A method for recording behavior and multineuronal CNS activity from tethered insects flying in virtual space. *Journal of Neuroscience Methods*, *120*, 211–223.
- Haag, J., & Borst, A. (1996). Amplification of high frequency synaptic inputs by active dendritic membrane processes. *Nature*, *379*, 639–641.
- Haag, J., & Borst, A. (1997). Encoding of visual motion information and reliability in spiking and graded potential neurons. *Journal of Neuroscience*, *17*, 4809–4819.
- Haag, J., & Borst, A. (1998). Active membrane properties and signal encoding in graded potential neurons. *Journal of Neuroscience*, *18*, 7972–7986.
- Haag, J., & Borst, A. (2000). Spatial distribution and characteristics of voltage-gated calcium signals within visual interneurons. *Journal of Neurophysiology*, *83*, 1039–1051.
- Haag, J., & Borst, A. (2001). Recurrent network interactions underlying flow-field selectivity of visual interneurons. *Journal of Neuroscience*, *21*, 5685–5692.
- Haag, J., Theunissen, F., & Borst, A. (1997). The intrinsic electrophysiological characteristics of fly lobula plate tangential cells: II. Active membrane properties. *Journal of Computational Neuroscience*, *4*, 349–369.
- Haag, J., Vermeulen, A., & Borst, A. (1999). The intrinsic electrophysiological characteristics of fly lobula plate tangential cells: III. Visual response properties. *Journal of Computational Neuroscience*, *7*, 213–234.
- Harris, R. A., & O'Carroll, D. C. (2002). Afterimages in fly motion vision. *Vision Research*, *42*, 1701–1714.
- Harris, R. A., O'Carroll, D. C., & Laughlin, S. B. (1999). Adaptation and the temporal delay filter of fly motion detectors. *Vision Research*, *39*, 2603–2613.
- Harris, R. A., O'Carroll, D. C., & Laughlin, S. B. (2000). Contrast gain reduction in fly motion adaptation. *Neuron*, *28*, 595–606.
- Hausen, K. (1982a). Motion sensitive interneurons in the optomotor system of the fly. I. The Horizontal Cells: Structure and signals. *Biological Cybernetics*, *45*, 143–156.
- Hausen, K. (1982b). Motion sensitive interneurons in the optomotor system of the fly. II. The Horizontal Cells: Receptive field organization and response characteristics. *Biological Cybernetics*, *46*, 67–79.
- Hausen, K., & Egelhaaf, M. (1989). Neural mechanisms of visual course control in insects. In D. Stavenga, & R. C. Hardie (Eds.), *Facets of vision* (pp. 391–424). Berlin, Heidelberg, New York: Springer.
- Hengstenberg, R. (1977). Spike responses of 'non-spiking' visual interneurone. *Nature*, *270*, 338–340.
- Horstmann, W., Egelhaaf, M., & Warzecha, A.-K. (2000). Synaptic interactions increase optic flow specificity. *European Journal of Neuroscience*, *12*, 2157–2165.
- Juusola, M., French, A. S., Uusitalo, R. O., & Weckström, M. (1996). Information processing by graded-potential transmission through tonically active synapses. *Trends in Neurosciences*, *19*, 292–297.
- Kent, J. (1993). The flic file format. *Dr Dobb's Journal*, *18*, 18–22.
- Kern, R., Lutterklas, M., & Egelhaaf, M. (2000). Neural representation of optic flow experienced by unilaterally blinded flies on their mean walking trajectories. *Journal of Comparative Physiology A*, *186*, 467–479.

- Kern, R., Lutterklas, M., Petereit, C., Lindemann, J. P., & Egelhaaf, M. (2001a). Neuronal processing of behaviourally generated optic flow: Experiments and model simulations. *Network: Computations in Neural Systems*.
- Kern, R., Petereit, C., & Egelhaaf, M. (2001b). Neural processing of naturalistic optic flow. *Journal of Neuroscience*, *21*, 1–5.
- Krapp, H. G., Hengstenberg, R., & Egelhaaf, M. (2001). Binocular contribution to optic flow processing in the fly visual system. *Journal of Neurophysiology*, *85*, 724–734.
- Laughlin, S. B. (1994). Matching coding, circuits, cells, and molecules to signals: General principles of retinal design in the fly's eye. *Progress in Retinal and Eye Research*, *13*, 165–196.
- Lewen, G. D., Bialek, W., & de Ruyter van Steveninck, R. (2001). Neural coding of naturalistic motion stimuli. *Network: Computations in Neural Systems*, *12*, 317–329.
- Maddess, T., & Laughlin, S. B. (1985). Adaptation of the motion-sensitive neuron H1 is generated locally and governed by contrast frequency. *Proceedings of the Royal Society of London B*, *225*, 251–275.
- Passaglia, C., Dodge, F., Herzog, E., Jackson, S., & Barlow, R. (1997). Deciphering a neural code for vision. *Proceedings of the National Academy of Sciences of the United States of America*, *94*, 12649–12654.
- Pekel, M., Lappe, M., Bremmer, F., Thiele, A., & Hoffmann, K.-P. (1996). Neuronal responses in the motion pathway of the macaque monkey to natural optic flow stimuli. *Neuroreport*, *7*, 884–888.
- Petrowitz, R., Dahmen, H. J., Egelhaaf, M., & Krapp, H. G. (2000). Arrangement of optical axes and the spatial resolution in the compound eye of the female blowfly *Calliphora*. *Journal of Comparative Physiology A*, *186*, 737–746.
- Poggio, T., & Reichardt, W. (1973). Considerations on models of movement detection. *Kybernetik*, *13*, 223–227.
- Schilstra, C., & van Hateren, J. H. (1998). Using miniature sensor coils for simultaneous measurement of orientation and position of small, fast-moving animals. *Journal of Neuroscience Methods*, *83*, 125–131.
- Schilstra, C., & van Hateren, J. H. (1999). Blowfly flight and optic flow. I. Thorax kinematics and flight dynamics. *Journal of Experimental Biology*, *202*, 1481–1490.
- Sherk, H., & Fowler, G. A. (2001). Visual analysis and image motion in locomoting cats. *European Journal of Neuroscience*, *13*, 1239–1248.
- Simpson, J. I. (1984). The accessory optic system. *Annual Review of Neuroscience*, *7*, 13–41.
- Single, S., Haag, J., & Borst, A. (1997). Dendritic computation of direction selectivity and gain control in visual interneurons. *Journal of Neuroscience*, *17*, 6023–6030.
- Smakman, J. G. J., van Hateren, J. H., & Stavenga, D. G. (1984). Angular sensitivity of blowfly photoreceptors: Intracellular measurements and wave-optical predictions. *Journal of Comparative Physiology A*, *155*, 239–247.
- Strauss, R., Schuster, S., & Götz, K. G. (1997). Processing of artificial visual feedback in the walking fruit fly *Drosophila melanogaster*. *Journal of Experimental Biology*, *200*, 1281–1296.
- van Hateren, J. H., & Schilstra, C. (1999). Blowfly flight and optic flow. II. Head movements during flight. *Journal of Experimental Biology*, *202*, 1491–1500.
- van Hateren, J. H., & Snippe, H. P. (2001). Information theoretical evaluation of parametric models of gain control in blowfly photoreceptor cells. *Vision Research*, *41*, 1851–1865.
- Vinje, W. E., & Gallant, J. L. (2000). Sparse coding and decorrelation in primary visual cortex during natural vision. *Science*, *287*, 1273–1276.
- Vinje, W. E., & Gallant, J. L. (2002). Natural stimulation of the nonclassical receptive field increases information transmission efficiency in V1. *Journal of Neuroscience*, *22*, 2904–2915.
- Warzecha, A.-K., Egelhaaf, M., & Borst, A. (1993). Neural circuit tuning fly visual interneurons to motion of small objects. I. Dissection of the circuit by pharmacological and photoinactivation techniques. *Journal of Neurophysiology*, *69*, 329–339.
- Warzecha, A.-K., Kretzberg, J., & Egelhaaf, M. (1998). Temporal precision of the encoding of motion information by visual interneurons. *Current Biology*, *8*, 359–368.